

# **A Practical Guide for Selecting and Utilizing Pulsars for Galactic Navigation**

**Richard A. Russel**  
**Deep Space Exploration Society**

## **Abstract**

This paper describes an approach to select pulsars that are visible along the path of a theoretical galactic spacecraft. The method includes determining the galactic angles relative to the rotating “lighthouse” beam as well as the use of the time delayed pulsar period to determine the spacecraft distance from the pulsar. The methods described are used for a hypothetical trip between two points in the galaxy.

## **1. Pulsar Galactic Navigation Theory**

Galactic navigation requires the use of a common three- dimensional reference (X, Y, Z) frame referred to as the galactic – center frame. In this frame the center of the galaxy is at (0,0,0). The Sun is approximately at (0, 8500 pc, 0) (Russel, Galactic Navigation Position Data Using HI Interstellar Medium Velocity Measurements, 2018) (Russel, Earth's Orbital Position in the Solar System using Galactic HI Measurements, 2019) (Russel, Milky Way Rotation Rate and Mass Estimation using HI Measurements, 2019). Pulsars can be plotted using the same galactic framework and therefore provide a geometric relationship that can be used to triangulate navigational positions. Pulsars also have a unique property based on the radio observable rotation rate. This rate provides a unique identifier for each pulsar and also a unique spin-down rate. The distance from the pulsar can be estimated using the observable spin-rate and then calculating the distance and therefore time based on the speed of light that it would take for the pulsar rate to be observed. (Lyne & Graham-Smith, 1990) (Lorimer & Kramer, 2005)

By developing distance solutions for multiple pulsars, it is possible to develop a model that estimates the 3 – dimensional galactic coordinates of the spacecraft. Once the model is developed the basic guide for a galactic navigator includes:

- Determine the starting point and destination galactic coordinates
- Determine the points between the start and destination that pulsar observations will need to be taken for navigation
- Determine which pulsars are visible at the navigation points
- Select the pulsars that give the small error at each navigation point (preflight)
- During flight – stop and take pulsar period observations and use the model to solve the galactic coordinate position
- Adjust course accordingly and restart flight to the next navigation point.

## **2. Pulsar Geometry**

A pulsar is formed during the collapse of a larger star. As the star collapses the new neutron star spins faster to retain its angular momentum. The neutron star is formed with a magnetic field that has an offset from the spin axis. The magnetic field emits a radio signal that can be detected like a lighthouse by the radio telescopes. (Figure 1) The offset angle causes the radio signal to “pulse” with a detectable spin rate. The magnetic field also causes a braking effect on the pulsar spin rate. This spin-down rate can therefore be used to predict the pulsar spin rate over time. (Lyne & Graham-Smith, 1990) (Lorimer & Kramer, 2005)

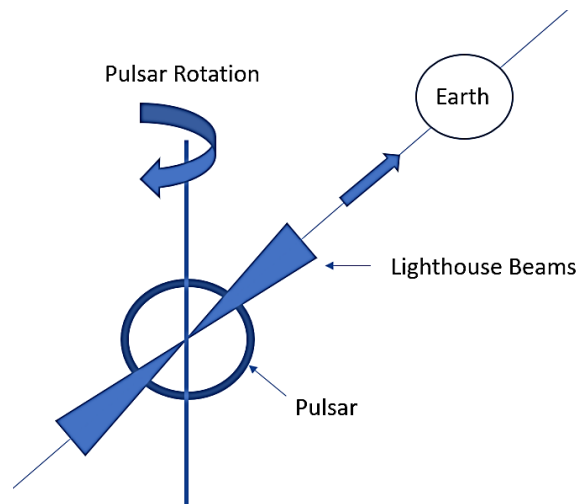



Figure 1: Pulsar Geometry

A list of pulsars can be found at the Australia Telescope National Facility (Australia Telescope National Facility, n.d.) (Figure 2) and at the VizieR database (Pulsar Catalog) (Manchester, Hobbs, A., & Hobbs, 2006)(Figure 3).



ATNF Pulsar Catalogue

Catalogue Version: 1.60

#	PSRJ		G1 (deg)	Gb (deg)	P0 (s)		P1		DIST (kpc)
1	J0002+6216	<a href="#">cwp+17</a>	117.327	-0.074	0.1153635682680	14	<a href="#">cwp+17</a>	5.96703E-15	7 <a href="#">cwp+17</a> *
2	J0006+1834	<a href="#">cnt96</a>	108.172	-42.985	0.69374767047	14	<a href="#">cn95</a>	2.097E-15	12 <a href="#">cn95</a> 0.86
3	J0007+7303	<a href="#">aaa+09c</a>	119.660	10.463	0.3158731909	3	<a href="#">awd+12</a>	3.6039E-13	5 <a href="#">awd+12</a> 1.40
4	J0011+08	<a href="#">dsm+16</a>	106.228	-53.407	2.55287	0	<a href="#">dsm+16</a>	*	0 * 5.40
5	J0014+4746	<a href="#">dth78</a>	116.497	-14.631	1.240699038946	11	<a href="#">h1k+04</a>	5.6446E-16	14 <a href="#">h1k+04</a> 1.78
6	J0023+0923	<a href="#">hrm+11</a>	111.383	-52.849	0.003050203104480002	7	<a href="#">abb+18</a>	1.14234E-20	4 <a href="#">abb+18</a> 1.11
7	J0024-7204aa	<a href="#">ph1+16</a>	305.895	-44.889	0.00184	0	<a href="#">ph1+16</a>	*	0 * 2.69
8	J0024-7204ab	<a href="#">ph1+16</a>	305.891	-44.891	0.0037046394947985	6	<a href="#">frk+17</a>	9.820E-21	9 <a href="#">frk+17</a> 2.54
9	J0024-7204C	<a href="#">mld+90</a>	305.923	-44.892	0.00575677999551635	14	<a href="#">frk+17</a>	-4.98503E-20	20 <a href="#">frk+17</a> 4.69
10	J0024-7204D	<a href="#">mlr+91</a>	305.881	-44.893	0.00535757328486573	9	<a href="#">frk+17</a>	-3.4220E-21	9 <a href="#">frk+17</a> 4.69
11	J0024-7204E	<a href="#">mlr+91</a>	305.883	-44.883	0.00353632915276244	4	<a href="#">frk+17</a>	9.85103E-20	6 <a href="#">frk+17</a> 4.69
12	J0024-7204F	<a href="#">mlr+91</a>	305.899	-44.892	0.00262357935251262	4	<a href="#">frk+17</a>	6.45029E-20	7 <a href="#">frk+17</a> 4.69
13	J0024-7204G	<a href="#">rlm+95</a>	305.891	-44.893	0.00404037914356515	14	<a href="#">frk+17</a>	-4.21584E-20	17 <a href="#">frk+17</a> 4.69
14	J0024-7204H	<a href="#">mlr+91</a>	305.896	-44.902	0.00321034070935032	11	<a href="#">frk+17</a>	-1.8294E-21	11 <a href="#">frk+17</a> 4.69
15	J0024-7204I	<a href="#">mlr+91</a>	305.892	-44.893	0.00348499206166289	13	<a href="#">frk+17</a>	-4.5874E-20	3 <a href="#">frk+17</a> 4.69

Figure 2: ATNF Pulsar Database (Australia Telescope National Facility, n.d.)



Figure 3: VizieR Database (SIMBAD Astronomical Database - CDS (Strasbourg), n.d.)

The data needed from these databases include galactic latitude and longitude, distance from Earth, period at Earth, and period spin-down rate ( $P_{\text{dot}}$ ).

### 3. Galactic Coordinate Navigation Model

The galactic coordinate navigation model is designed to determine a spacecrafts position as it transits from any two points in the galaxy. A theoretical faster than light (FTL) trip through the galaxy would require the spacecraft to drop out of FTL in order to detect the pulsars radio signal. Figure 4 shows the models 3 planned stopping points between a trip between Earth and Kepler 452b, which is a super-Earth detected by the Kepler spacecraft.

	Gal-X (pc) (Galactic-Centric)	Gal-Y (pc) (Galactic-Centric)	Gal-Z (pc) (Galactic-Centric)
Earth	0.00	8500.00	0.00
25%	103.47	8477.75	18.64
50%	206.94	8455.50	37.28
75%	310.41	8433.25	55.92
K452b	413.89	8411.00	74.55

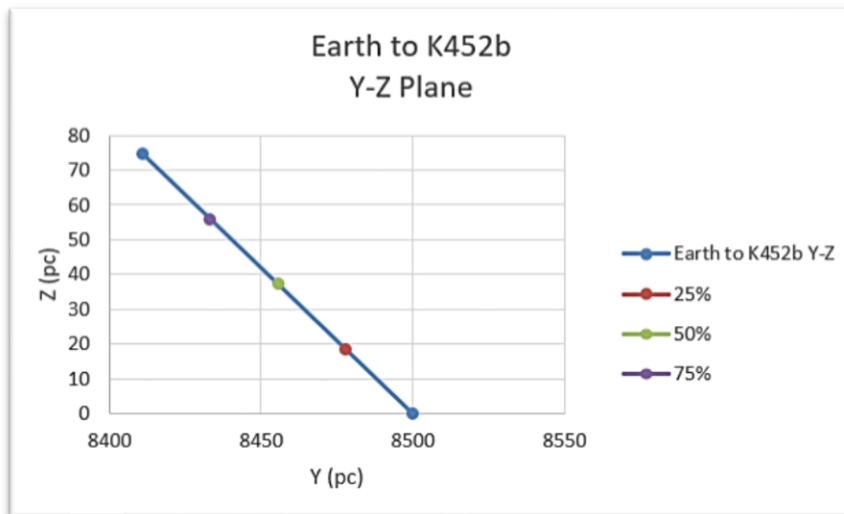
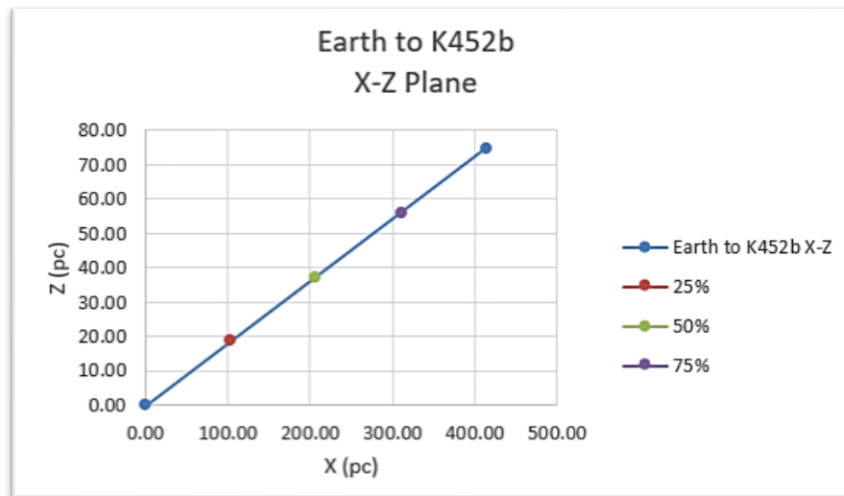
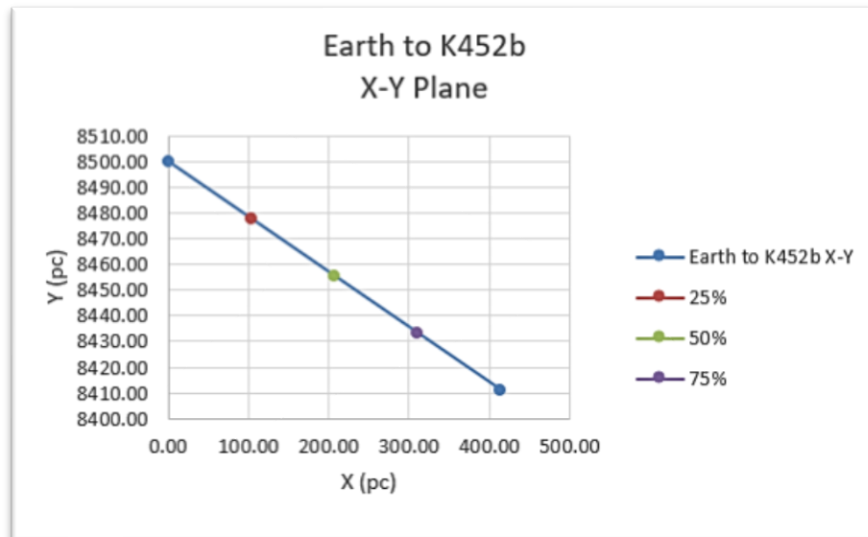
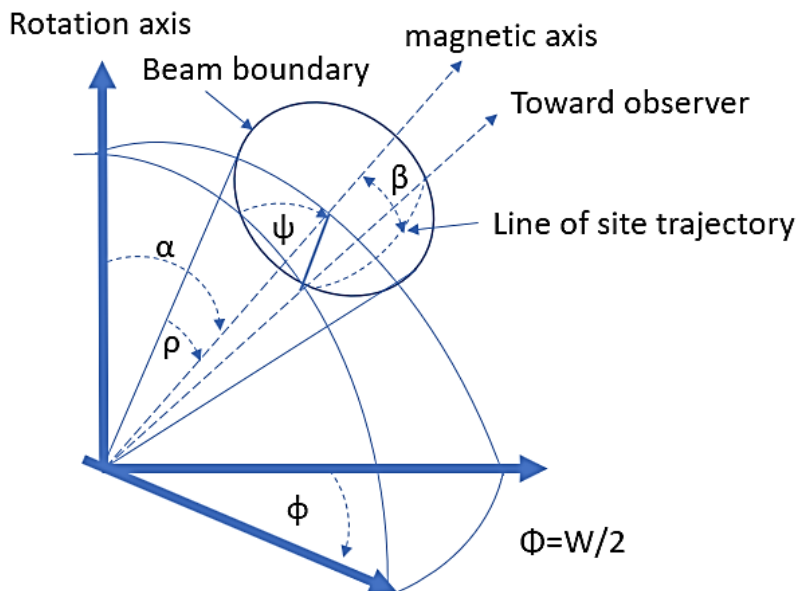


*Figure 4: Galactic-Centric Coordinates for Earth to K452b trip in the X-Y, X-Z, and Y-Z Plane*

The calculator provides an estimate along the path in (X, Y, Z) galactic -centric coordinates. Any percent of path can be calculated by simply changing the % value. The starting and ending points can be changed by entering in the three-dimensional coordinates.

#### 4. Model to Determine if Pulsars are Visible along the Flight Path

The nature of a pulsar is that the radio beam is not visible in all directions. The geometry of the beam is shown in Figure 5. (Lyne & Graham-Smith, 1990)



$\rho$ : beam angle  
 $\alpha$ : magnetic inclination angle  
 $\beta$ : impact angle  
 $W$ : observer pulse width

Figure 5: Pulsar Geometry (Lorimer & Kramer, 2005, p. 68)

The beam angle is estimated in equation (1) (Lorimer & Kramer, 2005, p. 70):

$$\rho \approx \frac{5.4 P^{-1/2}}{s} \quad (1)$$

The beam angle ( $\rho$ ) provides the basis for the model to determine if the path is in view of the pulsar.

- 1) The maximum value of  $2\rho$  is  $90^\circ$ . A larger angle would violate the light cylinder around the pulsar in which the magnetic field lines break before reaching the speed of light.
- 2) The Earth is within the  $2\rho$  angle because we currently observe the pulsar. The model assumes that the Earth is on the edge of the beam and that beam can be seen along the path across the entire  $2\rho$  angle. This is the worst-case high value; therefore, the model can limit the angle by any percent needed. However, for the following exercise, the entire  $2\rho$  value will be used for each pulsar.
- 3) Each pulsar will have a unique  $\rho$  angle based on its period. The model will show a green alert if a pulsar is visible along the path. The model can show the path position anywhere along the path. The entire pulsar database alerts for are then updated so that the visible pulsars can be selected.

A navigation path using a single pulsar is shown in Figure 6, The use of multiple pulsars that also have visibility throughout the trip, provides greater navigation accuracy and ambiguity resolution.

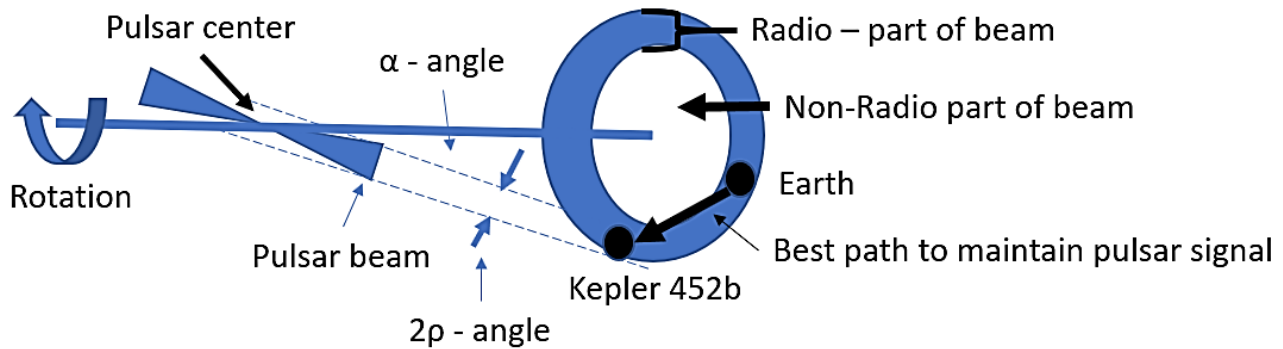
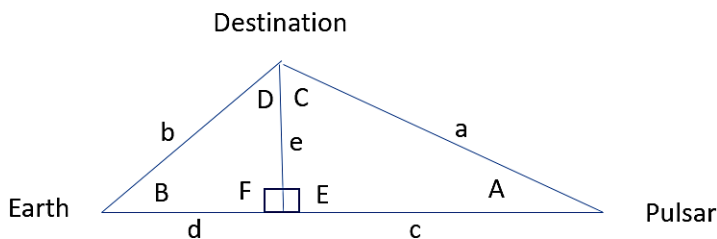


Figure 6: Best Spacecraft Path to Maintain Contact with Pulsar

The Earth, destination, and pulsar form a triangle for each plane (Figure 7). The database provides the estimated distances from the Earth and pulsar (line c-d). The distance between the Earth – destination (line b), and pulsar – destination (line a) are easily calculated. The important angle is angle A. This is the angle that corresponds to the 2p beam angle of the pulsar. If angle A is < 2p then the pulsar should be visible at the destination. Figure 7 shows the derivation of the angle A value. This was used in the model and compared to the 2p angle for each of the three planes.



$$\frac{c+d}{a} = \frac{a}{c} \quad \text{P 105 Geometry Cliff Notes}$$

$$c = \frac{a^2}{c+d}$$

$$d = (c+d) - c$$

$$e = \sqrt{a^2 - c^2}$$

$$A = \text{ASIN}\left(\frac{e}{a}\right)$$

$$B = \text{ACOS}\left(\frac{d}{b}\right)$$

$$C = \text{ASIN}\left(\frac{c}{a}\right)$$

$$D = \text{ASIN}\left(\frac{d}{b}\right)$$

- a: Pulsar to Destination Distance – known
- b: Earth to Destination Distance – known
- c+d: Earth to Pulsar Distance – known
- e: Base Height
- A: Earth – Pulsar - Destination Angle – unknown
- B: Pulsar –Earth –Destination Angle – unknown
- C+D: Pulsar – Destination –Earth Angle - unknown
- E & F: 90 degree Angles by definition

Figure 7: Angle Geometry

The master pulsar database automatically calculates the geometry of the pulsar to the navigation point and calculates three angles. If the angles are less than the 2p angle, they are colored green, otherwise they are colored red (Figure 8).

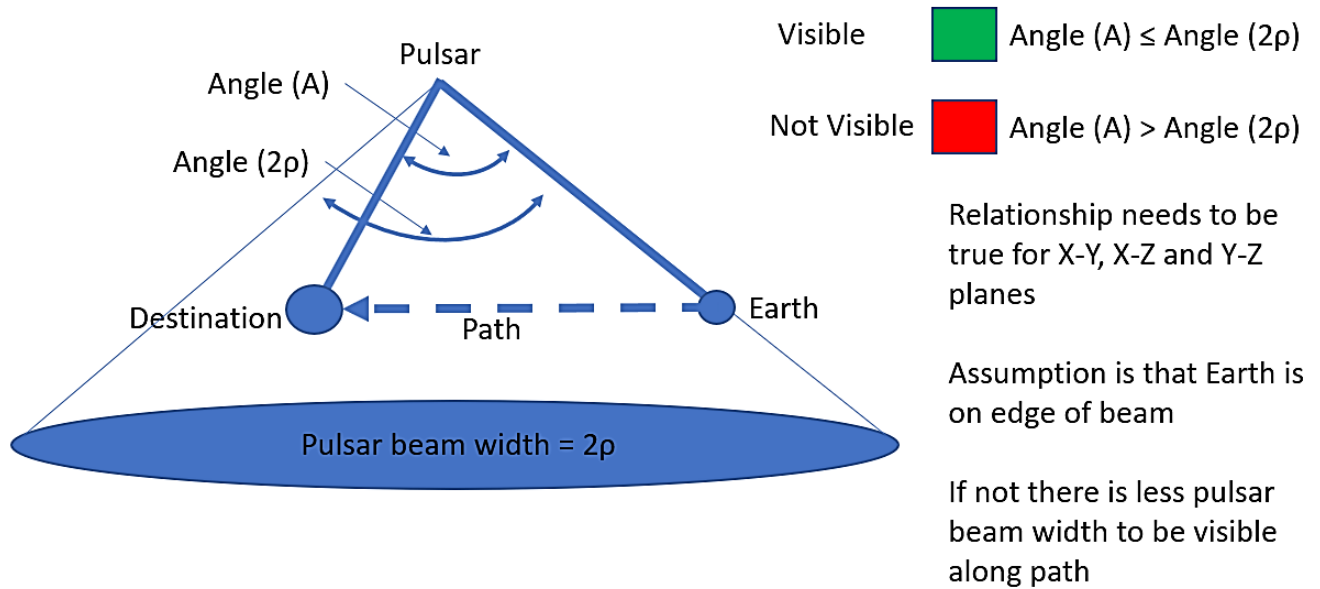
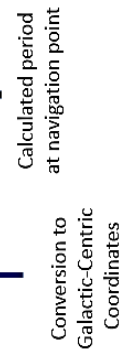


*Figure 8: Geometry to predict if pulsar beam can be seen along path*

The calculations of angles were added to the master pulsar database. This provides a quick reference for the selection of pulsars that are visible at any position in the galaxy. (Figure 9)

Figure 9: Master Pulsar Model





The pulsars that are visible can now be defined. The next step is to select the pulsars and use their periods and  $P_{\text{dot}}$  values to calculate the 3-dimensional galactic coordinates. The pulsars that meet the requirements of having a beam of  $2p$  diameter beam width that is visible along the entire path are shown in Figure 10.

ATNF Pulsar Line #	Jname	Glong (l)	Glat (b)	Dist (kpc)	Po (s)	Pdot	X(pc)	Y(pc)	Z(pc)	Base Period (s)	Expected Period at pt (seconds)	p	ATNF Pulsar Line #	X-Y 2p=angle (A)?	X-Z 2p=angle (A)?	Y-Z 2p=angle (A)?
6	0023+0923	113.38	-52.85	1.11	0.003050203	1.14234E-20	624.2	8744.4	-884.7	0.00305020	0.00305020	90.0	6	144.7	140.7	144.8
119	0337+1715	189.99	-30.94	1.30	0.002732589	1.77E-20	195.6	9608.3	-650.8	0.00273259	0.00273259	90.0	119	174.2	169.5	170.8
272	0721-2038	234.67	-2.92	2.98	0.015542395	4.40E-20	-2183.6	10047.8	-136.6	0.01554241	0.01554239	43.3	272	68.9	45.3	79.7
1126	1643-1224	5.67	23.22	4.86	0.004621661	3.39E-20	447.6	3991.6	1758.9	0.00462166	0.00462164	79.4	1126	153.3	146.2	154.4
1626	1804-0735	28.79	6.77	3.10	0.023100555	4.75E-19	1092.7	5622.1	365.6	0.02310101	0.02310086	35.5	1626	60.1	42.8	65.9
2376	1932+2020	55.57	0.64	9.14	0.264216554	4.22E-15	7538.8	3333.2	101.9	0.27218064	0.26820933	30.4	2376	11.5	9.8	17.2
2575	2055+3630	79.11	-5.59	5.56	0.221508034	3.65E-16	5434.3	7456.8	-541.5	0.22171666	0.22151318	11.5	2575	10.1	10.1	19.8
2616	2149+6329	104.25	7.41	13.64	0.380140345	1.66E-16	13109.6	11830.5	1759.7	0.38037618	0.38014266	8.8	2616	9.5	9.2	15.7

Figure 10: Pulsars that meet the  $2p$  requirement along entire path

The X-Y plane position of the selected pulsars are shown in Figure 11.

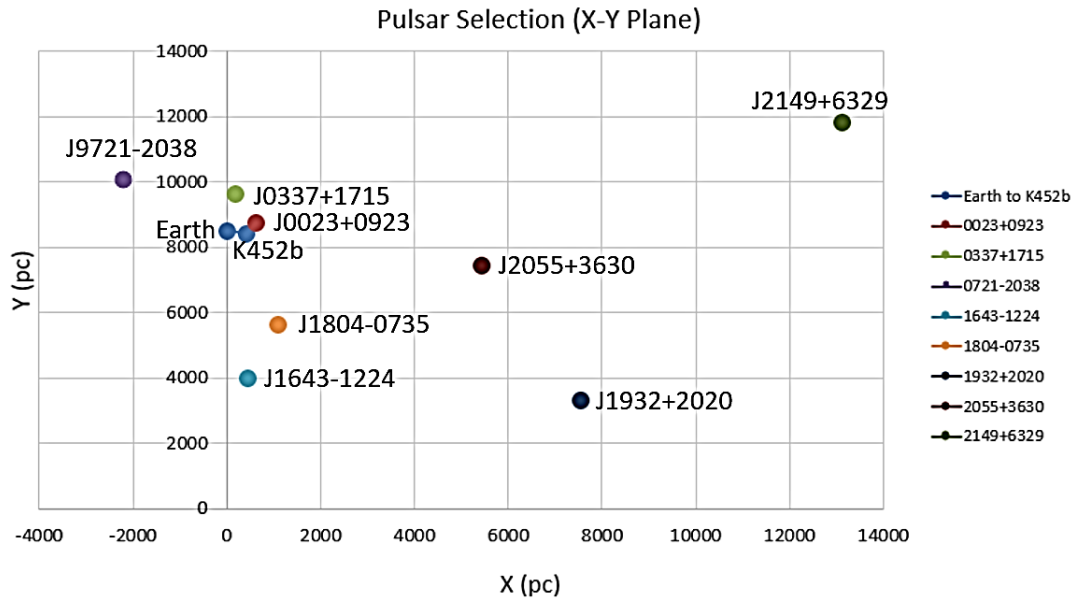


Figure 11: Pulsar Selection (X-Y Plane)

## 5. Math Model to Determine the Galactic Position

The following sequence of equations were used to establish a multiple equation and multiple unknown problem to determine the ship's galactic position by observing the pulsar periods during flight along the path. Equations 1-2 use the base period ( $P_{\text{base}}$ ) and spin down rate ( $P_{\text{dot}}$ ) to calculate a range from a pulsar to the ship's position based on an observed period of the pulsar ( $P_{\text{observed}}$ ).

$$P_{\text{base}} = P_{\text{observed}} + \dot{P}_{\text{dot}}(\text{distance in light years}) \quad (1)$$

$$\frac{P_{\text{base1}} - P_{\text{observed1}}}{\dot{P}_{\text{dot1}}} = \text{Pulsar 1 observed distance (LY)} \quad (2)$$

The EXCEL Solver program provides iterations on Trial X, Y, and Z galactic coordinates. The distance to the known pulsar to the Trial coordinates is calculated in Equations 3-5. Note that the actual model used 8 pulsars.

$$\sqrt{(\text{Trial } X - \text{Pulsar 1 } X)^2 + (\text{Trial } Y - \text{Pulsar 1 } Y)^2 + (\text{Trial } Z - \text{Pulsar 1 } Z)^2} = \text{Trial Pulsar 1 distance (LY)} \quad (3)$$

$$\sqrt{(Trial\ X - Pulsar\ 2\ X)^2 + (Trial\ Y - Pulsar\ 2\ Y)^2 + (Trial\ Z - Pulsar\ 2\ Z)^2} = Trial\ Pulsar\ 2\ distance\ (LY) \ (4)$$

$$\sqrt{(Trial\ X - Pulsar\ 3\ X)^2 + (Trial\ Y - Pulsar\ 3\ Y)^2 + (Trial\ Z - Pulsar\ 3\ Z)^2} = Trial\ Pulsar\ 3\ distance\ (LY) \ (5)$$

The difference error between the observed distance and the trial distance is calculated with equations 6-8.

$$Pulsar\ 1\ observed\ distance\ (LY) - Trial\ Pulsar\ 1\ distance\ (LY) = error\ 1 \ (6)$$

$$Pulsar\ 2\ observed\ distance\ (LY) - Trial\ Pulsar\ 2\ distance\ (LY) = error\ 2 \ (7)$$

$$Pulsar\ 3\ observed\ distance\ (LY) - Trial\ Pulsar\ 3\ distance\ (LY) = error\ 3 \ (8)$$

The EXCEL solver iterates the Trial X, Y, and Z coordinates until it reduces the sum of the errors to 0 or runs out of iterations. (Equation 9).

$$Solver\ set\ to\ find\ solution\ so\ that: error\ 1 + error\ 2 + error\ 3 = 0 \ (9)$$

## 6. Using Pulsar Period and Pulsar Spin down rate to determine distance to a pulsar.

A model was developed in EXCEL to meet the following requirements:

- Observe the pulsar period at the spacecraft position
- Determine the distance from the pulsar using the difference between the base period and the observed period.
- Use multiple pulsar observations to refine position.
- The following model was developed to determine the 3-dimensional galactic-Centric position using multiple pulsar measurements. (Figure 12)

# Solver Model to Calculate Distances

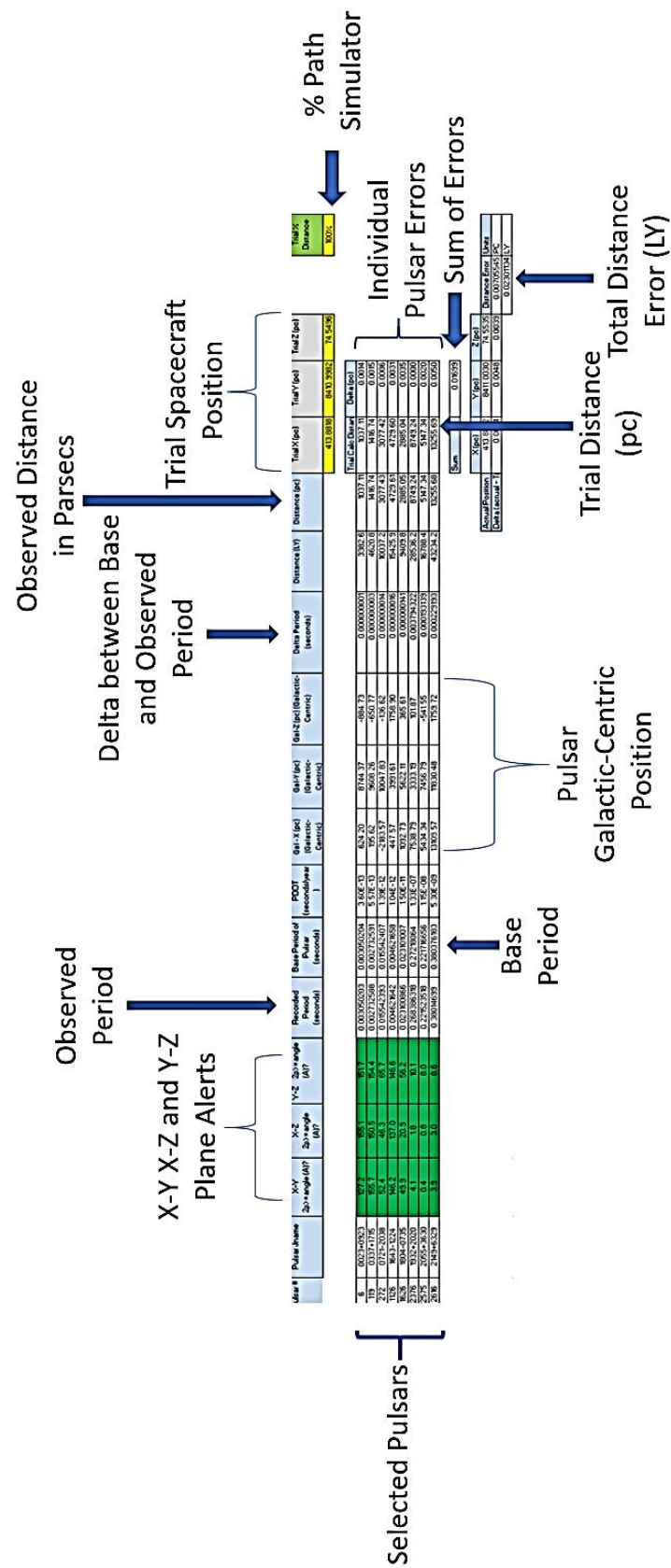


Figure 12: Pulsar Navigation Model

The Excel Solver program was used to calculate the best solution. Figure 13 shows the solver setup with the options selection that provided increased accuracy to the solution.

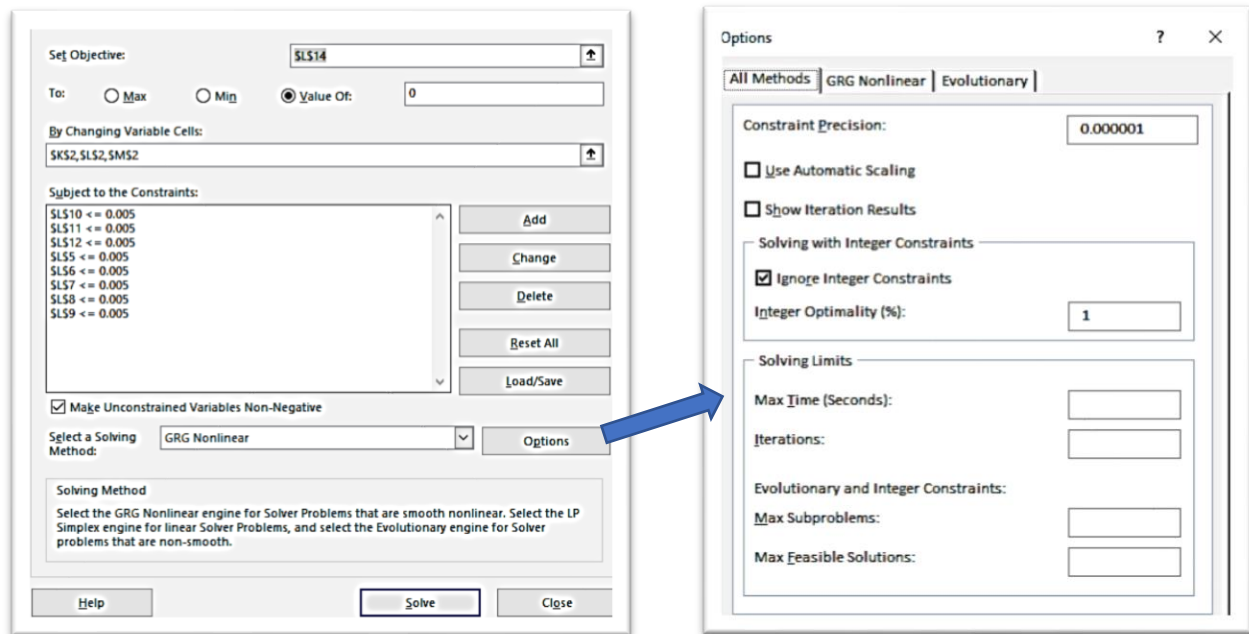


Figure 13: Solver Parameters

## 7. Error Analysis

The solver accuracy was tested using known values of the path galactic coordinates. The accuracy was tested by increasing the number of pulsars used in the solution. The results are shown in Figure 14.

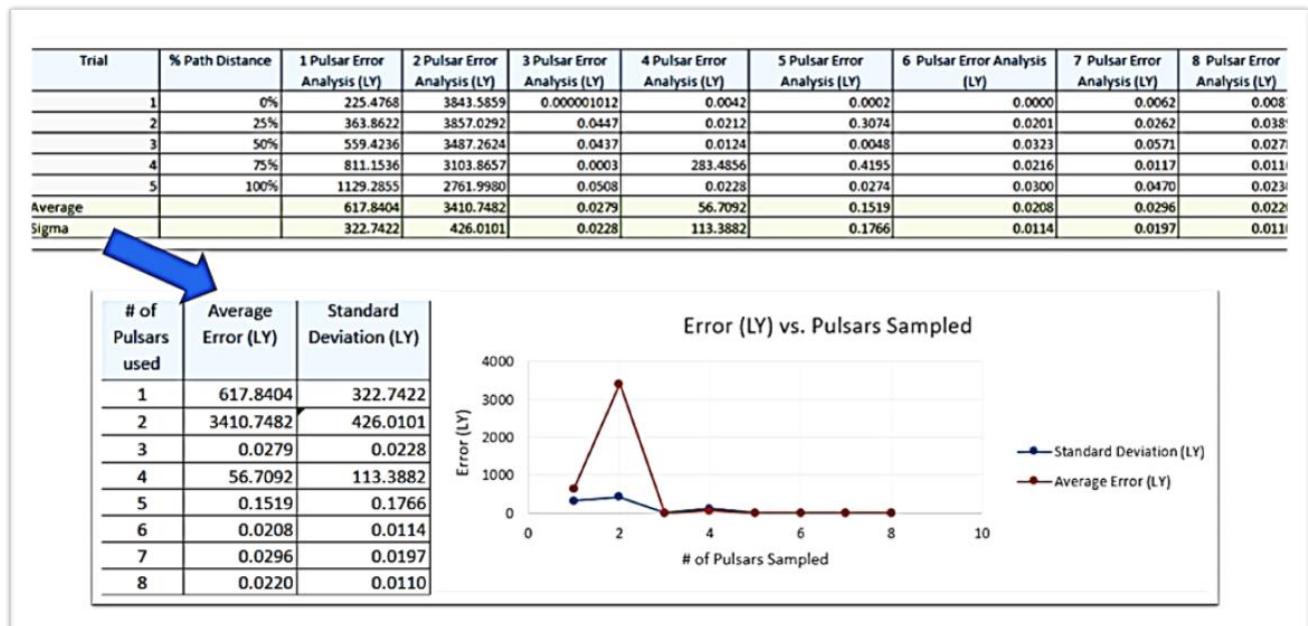


Figure 14: Error Analysis

The error analysis indicates that the model requires at least three pulsars to get accurate results. Figure 15 shows the relative distance that the error indicates. With an 8-pulsar observation, the solar system can be found compared to the next closest solar system, Alpha Centauri. The error should be able to be reduced using a better solver program. This will be explored in future research.

Location	Distance From Sun (km)	Distance from Sun (LY)
Jupiter	778,000,000	0.000082
Pluto	5,906,376,272	0.000624
Edge of Solar System	9,000,000,000	0.000951
8 Pulsar Error	208,016,924,775	0.021986
Alpha Centauri	41,345,737,565,365	4.370000

*Figure 15: Relative Distances Compared to Error Distance from Sun*

### 8. Planning the Galactic Trip using Pulsar Navigation

Using the above models, the following steps can be used to plan the galactic navigation using pulsars.

- Determine the start and destination of the galactic trip
- Determine the location of the path stops to obtain navigation data
- Based on the path stop location, determine which pulsars meet the alpha angle criteria (visible to the spacecraft at the stop point)
- Select Pulsars that have beams that intersect the path
- Select pulsars that provide a minimal AOU along the path
- Identify multiple points along the path to stop and take navigation data – FTL flight will not allow pulsar observation
- Adjust course and speed based on updated navigation position.
- Secondary – look for new pulsars that may not have been observable from Earth before.

#### Plan

- Plot path using galactic coordinates
- Choose pulsars that are visible along entire path

#### Underway Observations

- Stop and take observations
- Calculate new position
- Make course corrections accordingly

### 9. Practical example of a flight from Earth to Kepler 452b

The flight path from Earth to Kepler 452b is set up with three stops for navigation observations at 25%, 50% and 75% along the path. The model calculates the expected galactic coordinates at these points as shown in Figure 16. The coordinates are shown in the X-Y, X-Z, and Y-Z planes. Note that the 25% highlight in the model allows the path % to be transferred to the rest of the models features.

	Gal-X (pc) (Galactic-Centric)	Gal-Y (pc) (Galactic-Centric)	Gal-Z (pc) (Galactic-Centric)
Earth	0.00	8500.00	0.00
25%	103.47	8477.75	18.64
50%	206.94	8455.50	37.28
75%	310.41	8433.25	55.92
K452b	413.89	8411.00	74.55

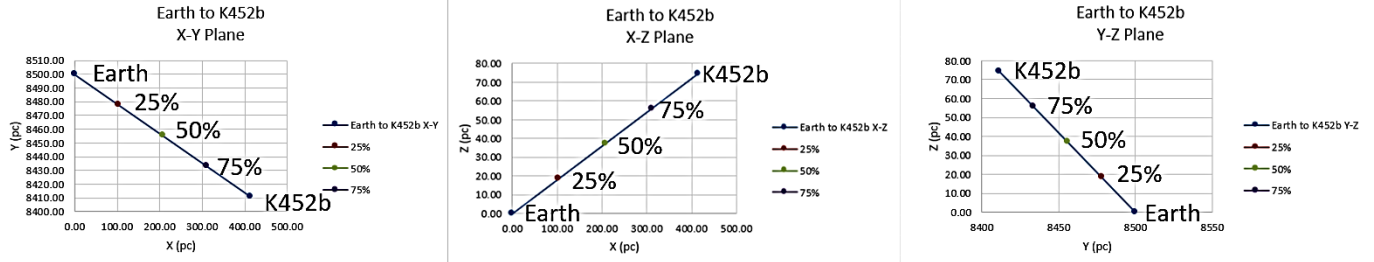


Figure 16: Planned Path in X-Y, X-Z, and Y-Z planes

Using the model's pulsar database, select pulsars that have a beam that encompasses the expected galactic position along the path. Note, that it is not necessary that the same pulsars be used along the entire path. Figure 17 shows the selected pulsars that meet the visibility path along the entire path.



ATNF Pulsar Line #	Jname	Glong (L)	Glat (b)	Dist (kpc)	Po (s)	Pdot	X(pc)	Y(pc)	Z(pc)	Base Period (s)	Expected Period at pt (seconds)	p	ATNF Pulsar Line #	X-Y 2p>angle (A)?	X-Z 2p>angle (A)?	Y-Z 2p>angle (A)?
6	0023+0923	111.38	-52.85	1.11	0.003050203	1.14234E-20	624.2	8744.4	-884.7	0.00305020	0.00305020	90.0	6	180.0	180.0	180.0
119	0337+1715	169.99	-30.04	1.30	0.002732589	1.77E-20	195.6	9608.3	-650.8	0.00273259	0.00273259	90.0	119	180.0	180.0	180.0
272	0721-2038	234.67	-2.92	2.68	0.015542395	4.40E-20	-2183.6	10047.8	-136.6	0.01554241	0.01554239	43.3	272	86.6	86.6	86.6
1126	1643-1224	5.67	21.22	4.86	0.004621641	3.30E-20	447.6	3991.6	1758.9	0.00462166	0.00462164	79.4	1126	158.9	158.9	158.9
1626	1804-0735	20.79	6.77	3.10	0.023100855	4.75E-19	1092.7	5622.1	365.6	0.02310101	0.02310086	35.5	1626	71.1	71.1	71.1
2376	1932+2020	55.57	0.64	9.14	0.268216854	4.22E-15	7538.8	3333.2	101.9	0.27218064	0.26821685	10.4	2376	20.9	20.9	20.9
2575	2055+3630	79.13	-5.59	5.56	0.221508034	3.65E-16	5434.3	7456.8	-541.5	0.22171666	0.22150803	11.5	2575	22.9	22.9	22.9
2616	2149+6329	104.25	7.41	13.64	0.380140345	1.68E-16	13109.6	11830.5	1759.7	0.38037618	0.38014034	8.8	2616	17.5	17.5	17.5

ATNF Pulsar Line #	Jname	Glong (L)	Glat (b)	Dist (kpc)	Po (s)	Pdot	X(pc)	Y(pc)	Z(pc)	Base Period (s)	Expected Period at pt (seconds)	p	ATNF Pulsar Line #	X-Y 2p>angle (A)?	X-Z 2p>angle (A)?	Y-Z 2p>angle (A)?
6	0023+0923	111.38	-52.85	1.11	0.003050203	1.14234E-20	624.2	8744.4	-884.7	0.00305020	0.00305020	90.0	6	150.8	164.4	166.7
119	0337+1715	169.99	-30.04	1.30	0.002732589	1.77E-20	195.6	9608.3	-650.8	0.00273259	0.00273259	90.0	119	172.8	173.9	167.7
272	0721-2038	234.67	-2.92	2.68	0.015542395	4.40E-20	-2183.6	10047.8	-136.6	0.01554241	0.01554239	43.3	272	70.8	68.4	76.5
1126	1643-1224	5.67	21.22	4.86	0.004621641	3.30E-20	447.6	3991.6	1758.9	0.00462166	0.00462164	79.4	1126	152.1	146.7	152.8
1626	1804-0735	20.79	6.77	3.10	0.023100855	4.75E-19	1092.7	5622.1	365.6	0.02310101	0.02310086	35.5	1626	60.1	46.5	63.6
2376	1932+2020	55.57	0.64	9.14	0.268216854	4.22E-15	7538.8	3333.2	101.9	0.27218064	0.26821685	10.4	2376	12.5	11.3	15.5
2575	2055+3630	79.13	-5.59	5.56	0.221508034	3.65E-16	5434.3	7456.8	-541.5	0.22171666	0.22151191	11.5	2575	11.7	11.9	15.2
2616	2149+6329	104.25	7.41	13.64	0.380140345	1.68E-16	13109.6	11830.5	1759.7	0.38037618	0.38014201	8.8	2616	10.7	10.3	13.3

ATNF Pulsar Line #	Jname	Glong (L)	Glat (b)	Dist (kpc)	Po (s)	Pdot	X(pc)	Y(pc)	Z(pc)	Base Period (s)	Expected Period at pt (seconds)	p	ATNF Pulsar Line #	X-Y 2p>angle (A)?	X-Z 2p>angle (A)?	Y-Z 2p>angle (A)?
6	0023+0923	111.38	-52.85	1.11	0.003050203	1.14234E-20	624.2	8744.4	-884.7	0.00305020	0.00305020	90.0	6	139.2	159.2	160.8
119	0337+1715	169.99	-30.04	1.30	0.002732589	1.77E-20	195.6	9608.3	-650.8	0.00273259	0.00273259	90.0	119	167.2	170.8	162.4
272	0721-2038	234.67	-2.92	2.68	0.015542395	4.40E-20	-2183.6	10047.8	-136.6	0.01554241	0.01554239	43.3	272	63.7	60.1	72.1
1126	1643-1224	5.67	21.22	4.86	0.004621641	3.30E-20	447.6	3991.6	1758.9	0.00462166	0.00462164	79.4	1126	149.5	142.2	150.2
1626	1804-0735	20.79	6.77	3.10	0.023100855	4.75E-19	1092.7	5622.1	365.6	0.02310101	0.02310086	35.5	1626	55.7	36.1	60.5
2376	1932+2020	55.57	0.64	9.14	0.268216854	4.22E-15	7538.8	3333.2	101.9	0.27218064	0.26830178	10.4	2376	9.0	7.4	13.9
2575	2055+3630	79.13	-5.59	5.56	0.221508034	3.65E-16	5434.3	7456.8	-541.5	0.22171666	0.22151579	11.5	2575	7.1	7.3	12.1
2616	2149+6329	104.25	7.41	13.64	0.380140345	1.68E-16	13109.6	11830.5	1759.7	0.38037618	0.38014367	8.8	2616	7.9	7.3	11.8

ATNF Pulsar Line #	Jname	Glong (L)	Glat (b)	Dist (kpc)	Po (s)	Pdot	X(pc)	Y(pc)	Z(pc)	Base Period (s)	Expected Period at pt (seconds)	p	ATNF Pulsar Line #	X-Y 2p>angle (A)?	X-Z 2p>angle (A)?	Y-Z 2p>angle (A)?
6	0023+0923	111.38	-52.85	1.11	0.003050203	1.14234E-20	624.2	8744.4	-884.7	0.00305020	0.00305020	90.0	6	131.2	156.3	156.0
119	0337+1715	169.99	-30.04	1.30	0.002732589	1.77E-20	195.6	9608.3	-650.8	0.00273259	0.00273259	90.0	119	161.5	160.6	158.2
272	0721-2038	234.67	-2.92	2.68	0.015542395	4.40E-20	-2183.6	10047.8	-136.6	0.01554241	0.01554239	43.3	272	57.8	53.0	68.7
1126	1643-1224	5.67	21.22	4.86	0.004621641	3.30E-20	447.6	3991.6	1758.9	0.00462166	0.00462164	79.4	1126	147.6	139.1	148.3
1626	1804-0735	20.79	6.77	3.10	0.023100855	4.75E-19	1092.7	5622.1	365.6	0.02310101	0.02310086	35.5	1626	52.5	28.0	58.2
2376	1932+2020	55.57	0.64	9.14	0.268216854	4.22E-15	7538.8	3333.2	101.9	0.27218064	0.26834410	10.4	2376	6.3	4.3	11.6
2575	2055+3630	79.13	-5.59	5.56	0.221508034	3.65E-16	5434.3	7456.8	-541.5	0.22171666	0.22151966	11.5	2575	3.4	3.8	9.8
2616	2149+6329	104.25	7.41	13.64	0.380140345	1.68E-16	13109.6	11830.5	1759.7	0.38037618	0.38014533	8.8	2616	5.8	5.0	9.8

ATNF Pulsar Line #	Jname	Glong (L)	Glat (b)	Dist (kpc)	Po (s)	Pdot	X(pc)	Y(pc)	Z(pc)	Base Period (s)	Expected Period at pt (seconds)	p	ATNF Pulsar Line #	X-Y 2p>angle (A)?	X-Z 2p>angle (A)?	Y-Z 2p>angle (A)?
6	0023+0923	111.38	-52.85	1.11	0.003050203	1.14234E-20	624.2	8744.4	-884.7	0.00305020	0.00305020	90.0	6	126.0	155.1	151.7
119	0337+1715	169.99	-30.04	1.30	0.002732589	1.77E-20	195.6	9608.3	-650.8	0.00273259	0.00273259	90.0	119	155.7	150.5	154.4
272	0721-2038	234.67	-2.92	2.68	0.015542395	4.40E-20	-2183.6	10047.8	-136.6	0.01554241	0.01554239	43.3	272	52.4	46.3	65.7
1126	1643-1224	5.67	21.22	4.86	0.004621641	3.30E-20	447.6	3991.6	1758.9	0.00462166	0.00462164	79.4	1126	146.2	137.0	146.9
1626	1804-0735	20.79	6.77	3.10	0.023100855	4.75E-19	1092.7	5622.1	365.6	0.02310101	0.02310087	35.5	1626	49.9	20.9	56.2
2376	1932+2020	55.57	0.64	9.14	0.268216854	4.22E-15	7538.8	3333.2	101.9	0.27218064	0.26838632	10.4	2376	4.1	1.8	10.1
2575	2055+3630	79.13	-5.59	5.56	0.221508034	3.65E-16	5434.3	7456.8	-541.5	0.22171666	0.22152352	11.5	2575	0.4	0.8	8.0
2616	2149+6329	104.25	7.41	13.64	0.380140345	1.68E-16	13109.6	11830.5	1759.7	0.38037618	0.38014699	8.8	2616	3.9	3.0	8.6

Earth

25%

50%

75%

K452b

Figure 17: Select Pulsars that are visible through Entire Path (All green)

During flight, the first stop at the 25% - point results in the following pulsar periods being observed. (Figure 18)

Pulsar #	Pulsar Jname	Recorded Period (seconds)
6	0023+0923	0.003050203
65	0117+5914	0.101501444
272	0721-2038	0.015542394
303	0808-3937	0.866343041
474	1057-5226	0.19702537
672	1326-6700	0.54294808
1112	1639-4604	0.264546471
1844	1832-1021	0.330384783

Figure 18: Pulsar Measurements at 25% Path Point

Run the Solver program for these pulsar periods to determine the spacecraft position. (Figure 19)

Observed Pulsar periods

Pulsar #	Pulsar Jname	Recorded Period (seconds)
6	0023+0923	0.003050203
119	0337+1715	0.002732589
272	0721-2038	0.015542394
1126	1643-1224	0.004621642
1626	1804-0735	0.023100858
2376	1932+2020	0.268269331
2575	2055+3630	0.22151318
2616	2149+6329	0.380142661

Solver Solution

Trial X (pc)	Trial Y (pc)	Trial Z (pc)
139.9948	8489.9997	15.0002

Pulsar #	Pulsar Jname	Recorded Period (seconds)	Base Period of Pulsar (seconds)	PDOT (seconds/year)	Gal - X (pc) (Galactic-Centric)	Gal - Y (pc) (Galactic-Centric)	Gal - Z (pc) (Galactic-Centric)	Delta Period (seconds)	Distance (LY)	Distance (pc)	Trial X (pc)	Trial Y (pc)	Trial Z (pc)
6	0023+0923	0.003050203	0.003050204	3.62E-13	624.20	8744.37	-884.73	0.000000001	3434.2	1052.94	139.9948	8489.9997	15.0002
119	0337+1715	0.002732589	0.002732591	5.57E-13	195.62	9608.26	-450.77	0.000000002	4248.6	1302.63	139.9948	8489.9997	15.0002
272	0721-2038	0.015542394	0.015542407	1.39E-12	-2183.57	12047.83	-136.62	0.000000013	9137.5	2801.57	139.9948	8489.9997	15.0002
1126	1643-1224	0.004621642	0.004621658	1.04E-12	447.57	3991.61	1758.90	0.000000016	15767.7	4834.38	139.9948	8489.9997	15.0002
1626	1804-0735	0.023100858	0.023101307	1.50E-11	1062.73	5622.11	365.61	0.000000149	9922.6	3042.27	139.9948	8489.9997	15.0002
2376	1932+2020	0.268269331	0.27218064	1.33E-07	7538.79	3333.19	101.87	0.003911309	28416.0	9019.00	139.9948	8489.9997	15.0002
2575	2055+3630	0.22151318	0.222176656	1.15E-08	5434.34	7456.79	-541.55	0.000203477	17687.0	5422.85	139.9948	8489.9997	15.0002
2616	2149+6329	0.380142661	0.380378183	9.82E-09	13109.97	11830.48	1739.72	0.000233522	44050.8	13506.02	139.9948	8489.9997	15.0002
Sum										0.02266			

Figure 19: Solver Solution to Observed Measurements

The trial position result is plotted in Figure 20 for the X-Y plane. Note, that the ship is off course! The navigator will need to plan a new course in order to hit the planned 50% point.



Solver position based  
on observed periods at 25% point

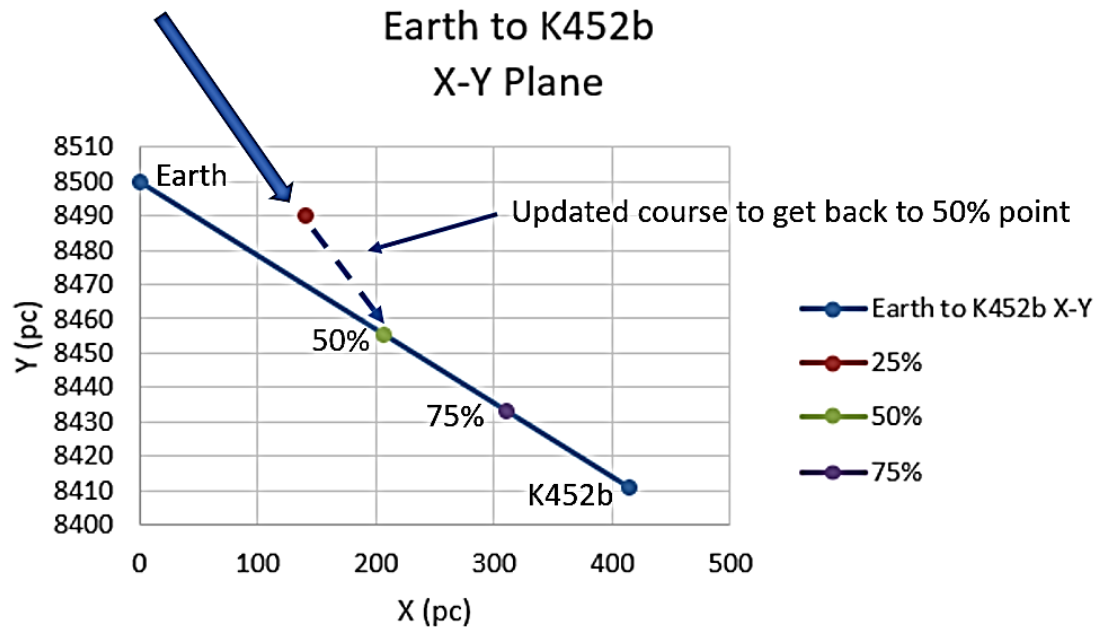


Figure 20: Observed position at 25% point

The X-Y, X-Z and Y-Z plane course adjustments are shown in figure 21.

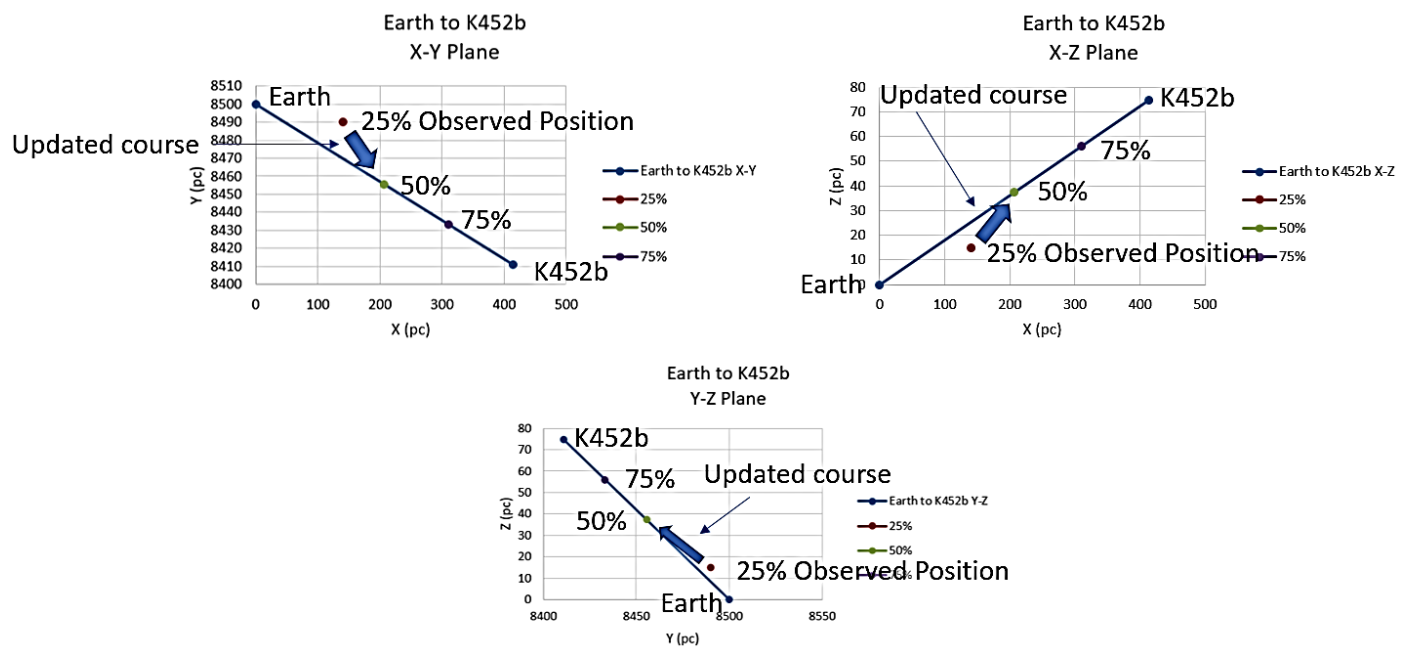


Figure 21: Course Updates Based on Observed Position

This process is completed as often as necessary in order to successfully use pulsars to navigate.

## **10. Follow-On work to improve the navigation accuracy**

The paper provides a basic approach to using pulsars to determine the galactic position using observed period measurements. The model is rudimentary and requires upgrades to reduce the error. These include:

- Characterize the beam cone in the model – this will provide better predictions of beam detection
- Get better pulsar spin down models that account for historical and predicted glitches and other timing anomalies.
- Add pulsar range errors: this will provide a more realistic area of uncertainty around the trial position.
- Develop a better “Solver” program to get a more precision that will allow for navigation within the solar system.
- Add GAIA astronomical catalog to improve accuracy of the galactic navigation data. GAIA provides positions, parallactic distances and proper motion for millions of galactic stars with precisions as good as a few micro-arcseconds. (Jones D. D., 2019)
- Each of the above Effects will only make small corrections to the Pulsar's Timing, but for Navigational purposes will become very important for long distance navigation.
  - 1. Doppler Shift Correction - the space craft is at a different Galactic Position and will be affected by the rotation of the Galaxy. (Boyd, 2019)
  - 2. Dispersion - As the RF signal passes through the ISM it will pass through different Interstellar Clouds causing time delay at the lower Pulsar frequencies. This needs to be corrected in order to detect the proper Pulsar. In some cases, the Dispersion can completely "smear out" the Pulsar's signal altogether. The Navigator could miss the chosen Pulsar. (Boyd, 2019)
  - 3. Lastly and most interesting is the effect of Gravity on measuring Time. As the space craft travels towards the Center of the Galaxy it will encounter a stronger Gravity Field. The Spacetime Curvature of the Gravitation Field will cause the Navigator's clock to change relative to the that of the Pulsar's. This is exactly what happens with GPS satellites at high altitudes above the Earth. So, a Relativistic Correction needs to be made by the Navigator. At the same time the Gravity Field can also be affected by any nearby locally massive object. So, it may be wise for the Navigator to choose waypoints that are not near any massive objects. The same effect works even when the space craft travels further away from the Galactic Center. (Boyd, 2019)

## **11. Summary**

The use of pulsars for galactic navigation is a viable option for futuristic FTL space flight. The precise measurements of the pulsar period and spin-down rate provide the ability to calculate distance to the pulsar. The distance of the pulsars from the Earth has a significant error range that needs to be refined. The agreement on the pulsar base period will also provide more accuracy to the trial range estimates. The calculated base periods for the ATNF database was calculated by the model and is available from the author.

## **12. Student Exercises using this Model**

The exercise of using pulsars for galactic navigation is an excellent way to teach the properties of pulsars, galactic coordinates, light speed, and modeling.

1) Take observed pulsar observations and determine the Earth's position. This is similar to using HI measurements to determine the Earth's position. (Russel, Earth's Orbital Position in the Solar System using Galactic HI Measurements, 2019)

2) Develop a pulsar message to another planetary system that uses only the pulsar periods observed from the Earth to provide a unique galactic position. This is similar to the Pioneer pulsar map which was developed by Frank Drake. (Russel, Galactic Navigation using the Pioneer Spacecraft Pulsar Map, 2019)

**Special Thanks:**

- The Deep Space Exploration Society ( [www.dses.science](http://www.dses.science) )
- Dr. Dayton Jones, Ralph Boyd, and Tony Bigbee for their excellent inputs on this article.
- Steve Plock and Jeffrey Lichtman for their continued support.

**For more information:**

Dr. Richard Russel [DrRichRussel@netscape.net](mailto:DrRichRussel@netscape.net)

Deep Space Exploration Society: [www.DSES.science](http://www.DSES.science)

**References**

- [1] Galactic Navigation Position Data Using HI Interstellar Medium Velocity Measurements. Russel, Richard A. s.l. : Proceedings of the Society of Amateur Radio Astronomers Western Regional Conference 2018, 2018.
- [2] Earth's Orbital Position in the Solar System using Galactic HI Measurements. Russel, Richard A. s.l. : Society of Amateur Radio Astronomers' Western Conference Proceedings, 2019. pp. 109-125.
- [3] Milky Way Rotation Rate and Mass Estimation using HI Measurements. Russel, Richard A. s.l. : Society of Amateur Radio Astronomers' Western Conference Proceedings, 2019. pp. 77-87.
- [4] Lyne, A.G. and Graham-Smith, F. Pulsar Astronomy. Cambridge : Cambridge University Press, 1990. ISBN 0 521 32681 8.
- [5] Lorimer, Duncan and Kramer, Michael. Handbook of Pulsar Astronomy. Cambridge : Cambridge University Press, 2005. ISBN 0 521 82823 6.
- [6] Australia Telescope National Facility. CASS Pulsar Group. [Online] <http://www.atnf.csiro.au/research/pulsar/index.html>.
- [7] Pulsar Catalog. VizierR.
- [8] AJ, 129, 1993-2006. Manchester, R. N., et al. 2006.
- [9] SIMBAD Astronomical Database - CDS (Strasbourg). [Online] <http://simbad.u-strasbg.fr/simbad/>.
- [10] Jones, Dr. Dayton. 2019.
- [11] Boyd, Ralph. 2019.
- [12] Galactic Navigation using the Pioneer Spacecraft Pulsar Map. Russel, Richard A. 2019, Radio Astronomy March - April 2019, pp. 49-59.



Dr. Rich Russel is the current science lead for the Deep Space Exploration Society. He is a retired Northrop Grumman Senior Systems Engineer and served as the Chief Architect for the Satellite Control Network Contract (SCNC). In this capacity he was charged with planning the future architecture of the Air Force Satellite Control Network (AFSCN) and extending the vision to the Integrated Satellite Control Network (ISCN). Dr. Russel has been the lead architect and integrator for the Space-Based Blue Force Tracking project for U.S Space Command, the Center for Y2K Strategic Stability, and CUBEL Peterson. Dr. Russel also has led the SPAWAR Factory team in the deployment of the UHF Follow-On

Satellite system. He has a Doctorate in Computer Science, an Engineers Degree in Aeronautics and Astronautics, a Master's in Astronautical Engineering, and a Bachelor's in Electrical Engineering. He is also certified as a Navy Nuclear Engineer and he is a retired Navy nuclear fast attack submariner and Navy Space Systems Engineer.